A single layer wideband metasurface absorber for electromagnetic interference minimization in Ku-band applications

Yogita Khanna[1] and Y. K. Awasthi[2] (iD)

[1]Electronics and Communication Engineering, Manav Rachna University, Faridabad, HR 121004, India and [2]Electronics and Communication Engineering, Manav Rachna International Institute of Research and Studies, Faridabad, HR 121004, India

CAMBRIDGE UNIVERSITY PRESS

Abstract

In this paper, a wideband ultrathin metasurface absorber is investigated. The proposed absorber comprises a periodic array of a unit cell ring structure. The ring structure and patch inside are tuned to realize the desired frequency bandwidth. The structure has a frequency bandwidth of 7.4 GHz with a center frequency of 15 GHz and fractional bandwidth of 50%. Simulated and measured results show that the absorption at normal incidence is above 90% in the frequency range of 11.3–18.7 GHz. Furthermore, the thickness of the structure is 1.6 mm. The physical mechanism of the metasurface absorber has been analyzed and justified experimentally.

Introduction

Microwave wideband absorbers provide numerous applications such as radar cross-sectional reduction and reduction of electromagnetic interference (EMI) between electronic equipment and stealth [1–5]. EMI problems caused by reflections due to metallic parts of the antenna of a ship or airplane radome are best controlled by absorbers covering a large range of frequency band on which the radars and antennas are intended [6, 7]. There are several approaches to increase the bandwidth of absorbers that have been published. A multi-layer structure increases the bandwidth of the absorber but simultaneously the thickness of the absorber also increases and the fabrication process becomes tough [8]. Another way of increasing the bandwidth of the absorber is using a magnetic medium but this increases the weight of absorbers, restricting their practical applications [9]. One convenient method is loading the structure with resistors or capacitors that increases the bandwidth to a large extent, but the value of the resistance is not variable, so it is difficult to obtain resistance suitable for different structures at different frequencies [5, 10, 11]. Therefore, searching for new methods that are easier to implement and use along with enhancing the bandwidth becomes a research focus. Metamaterial absorbers can be made ultra-thin as well as ultra-wideband with a high absorption rate if the structure is optimized for that specific band [2, 3, 12]. Several designs for metamaterial absorbers incorporating the advantages of polarization-insensitivity, incidence angle insensitivity, and ultra-wide bandwidth have been designed and examined [4, 7, 10, 11, 13–15]. Metamaterial absorber structures usually comprise a periodic array of top metallic patches and ground metal planes separated by a dielectric material.

The proposed absorber comprising a split-ring structure loaded with an inner floret-shaped patch is designed for enhancing the bandwidth only with a single layer FR-4 substrate. Simulation analysis of the proposed absorber is determined using the CST-Microwave Studio. The equivalent circuit for the overall impedance has been presented and the values of equivalent resistance, capacitance, and inductance at the center frequency are calculated. The designed absorber provides an alternative solution to the wideband absorbers that are bulky and expensive.

Design and equivalent circuit model

The metamaterial absorber design considered for the wide bandwidth consists of an array of circular ring structure that has split gaps and dielectric substrate that is grounded to block the transmission of electromagnetic waves as shown in Fig. 1(a).

The dielectric substrate used is the commercially available FR-4 ($\epsilon_r = 4.3$ and $\tan \delta = 0.02$) having a thickness of 1.6 mm. A top metallic patch having a circular ring structure and the bottom ground plane is constructed with copper having conductivity $\sigma = 5.8 \times 10^7$ S/m and thickness of 0.035 mm. Figure 1(a) shows the 3D view of the unit cell structure indicating the placement of the ground, substrate, and the patch for maximum absorption.
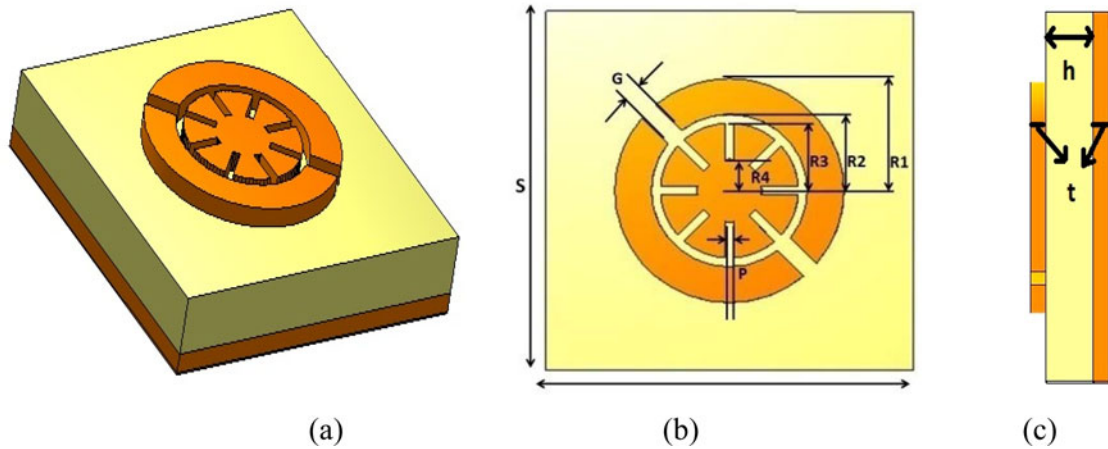
Fig. 1. Unit cell structure: (a) 3D view of the absorber unit cell, (b) the dimensions from the front view of the absorber, and (c) the dimensions from a side view.

Figure 1(b) indicates the detailed optimized dimensions of the patch on the top of the substrate. The spacing between the unit cells is given as $S = 6.8$ mm, the outer radius of a ring is given as $R1 = 2.5$ mm, and the inner radius $R2 = 1.7$ mm which indicates the ring width is 0.8 mm. The two split gaps given in the ring structure are denoted by $G = 0.4$ mm. Considering the inner floret patch the outer radius is $R3 = 1.5$ mm and the inner radius $R4 = 0.7$ mm. The eight split gaps of equal dimensions are given as $P = 0.2$ mm. Figure 1(c) shows the side view of the absorber structure which indicates the thickness of ground and patch as $t = 0.035$ mm and thickness of the substrate as $h = 1.6$ mm.

The absorption offered by an absorber $A(\omega)$ at various frequencies can be obtained by equation (1)

$$A(\omega) = 1 - R(\omega) - T(\omega) \qquad (1)$$

where $R(\omega)$ is the reflection coefficient and $T(\omega)$ is the transmission coefficient, and the copper ground plane ensures that there is no transmission through the absorber so the effective absorption offered is now obtained using equation (2)

$$A(\omega) = 1 - |S_{11}|^2 \qquad (2)$$

Simulations performed in CST-microwave studio provide the S-parameter values in the desired frequency sweep. The reflection coefficient includes both co-polarization and cross-polarization for transverse electric (TE) and transverse magnetic (TM) given in equation (3)

$$|S_{11}|^2 = |S_{11TE,TE}|^2 + |S_{11TE,TM}|^2 = |S_{11TM,TM}|^2 + |S_{11TM,TE}|^2 \quad (3)$$

where for TE as the incident wave $S_{11TE,\ TE}$ is co-polarization reflection coefficient and $S_{11TE,\ TM}$ indicates the cross-polarization reflection coefficient of the proposed design respectively. To confirm that the designed structure is not a polarization converter, the cross-polarization reflectivity is calculated.

The series equivalent circuit is approximated based on the resonator structure having R, L & C as the approximate values of resistance, inductance, and capacitance respectively. Z_{in} is the input impedance of the absorber, Z_m equivalent impedance of top layer of the proposed metasurface absorber, and Z_t is the
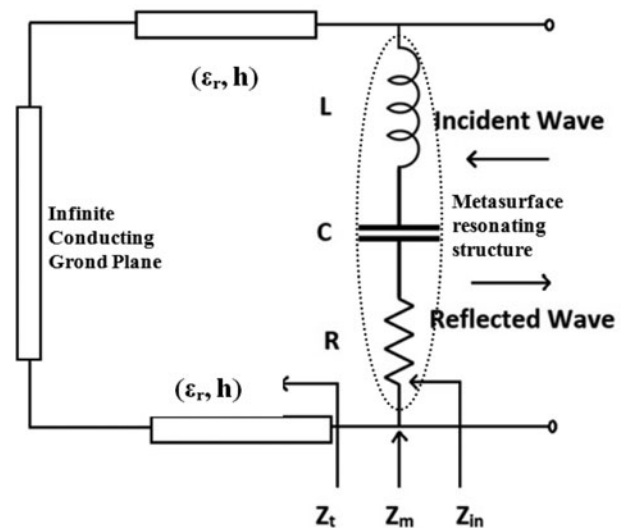

Fig. 2. Equivalent circuit for the absorber circuit for Resistance (R), Inductance (L) & Capacitance (C).

input impedance of dielectric metal surface or ground as given by equations (4)–(6) (Fig. 2):

$$\frac{1}{Z_{in}} = \frac{1}{Z_m} + \frac{1}{Z_t} \qquad (4)$$

$$Z_m = R + j\left(2\pi fL - \frac{1}{2\pi fC}\right) \qquad (5)$$

$$Z_t = j\frac{Z_0}{\sqrt{\varepsilon_r}}\tan\left(\frac{2\pi f \sqrt{\varepsilon_r}\, h}{c}\right) \qquad (6)$$

The circuit and equations thus analyzed for the maximum power transfer, where the impedance of free space shall be equal to the absorber impedance, gives the approximate values of R, L & C as
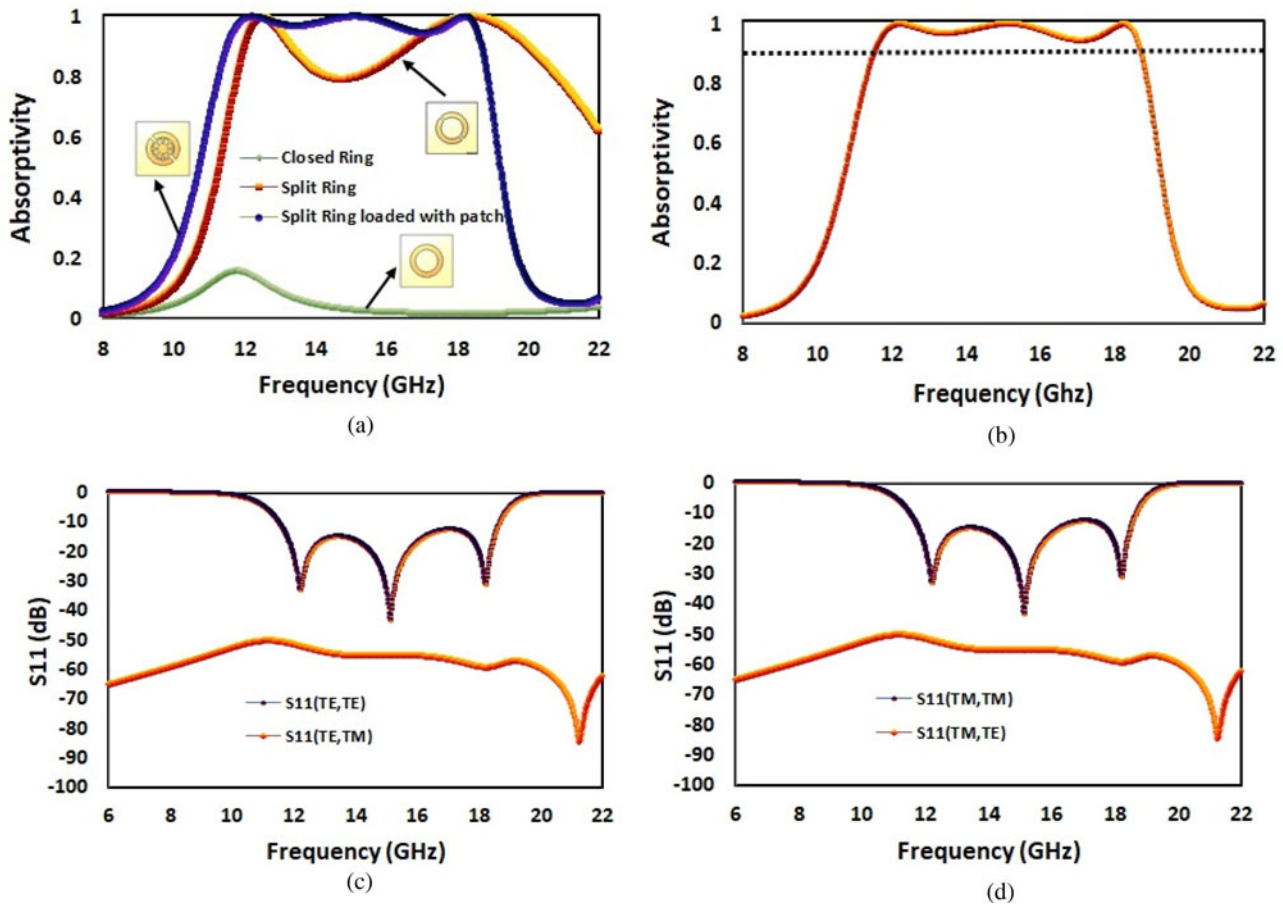
Fig. 3. Design phases of the absorber structure and absorptivity response of (a) a closed-loop ring, ring structure with split gaps i.e. split ring and split ring loaded with a patch, (b) absorptivity at normal incidence having a bandwidth of 7.4 GHz at 90% absorptivity (c) Reflection coefficient of co-polarization and (d) cross-polarization of TE and TM wave at normal incident.

given in equations (7)–(9):

$$R = \frac{Z_0 \tan^2\left(2\pi f \sqrt{\varepsilon_r} h/c\right)}{\varepsilon_r + \tan^2\left(2\pi f \sqrt{\varepsilon_r} h/c\right)} \qquad (7)$$

$$\left(2\pi f L - \frac{1}{2\pi f C}\right) = \frac{\sqrt{\varepsilon_r} Z_0 \tan\left(2\pi f \sqrt{\varepsilon_r} h/c\right)}{\varepsilon_r + Z_0 \tan^2\left(2\pi f \sqrt{\varepsilon_r} h/c\right)} \qquad (8)$$

$$L = 0.0002 \times l \times \left(2.303 \times \log_{10}\left(\frac{4 \times l}{t}\right) - \alpha\right) \mu H \qquad (9)$$

where the perimeter of circular ring $l = 2\pi R4$, conductor thickness $t = 0.035$ mm, and for circular-shaped ring structure value of α is 2.451.

## Absorber structure and parametric analysis

To analyze the structure for the design parameters, first, the basic structure design criteria are explained. Figure 3(a) indicates the various steps of designing the absorber structure and the absorptivity response in accordance. The initial structure is approximated from the L and C values calculated in Table 1 at the center frequency. The closed-loop structure shown in Fig. 3(a)

Table 1. Estimated values of R, L & C

ϵ_r	d (mm)	f (GHz)	R (Ω)	C (pF)	L (mH)
4.3	1.6	15	152	57.3	20.3

in the desired bandwidth has absorptivity below 20%. The structure is improved fairly by introducing the split gaps that increase the effective capacitance of the circuit. A floret-shaped structure is introduced in the absorber to increase the overall bandwidth of the structure through the multimode resonance mechanism. When a floret-shaped structure is merged with a split-ring resonator structure, the bandwidth variation is quite large when compared to the previous two cases. The bandwidth of the absorber is 7.4 GHz at 90% absorptivity as shown in Fig 3(b). Fig. 3(c) and 3(d) indicate the results obtained for the reflectivity for co-polarization and cross-polarization. From equation (2) the corresponding absorptivity is calculated.

The optimized structure is achieved from the parametric iteration for the desired results. Different parameters are varied one at a time while keeping the other parameters fixed as shown in Fig. 4. The unit cell spacing "S" is a critical parameter that responds to the achievement of desired bandwidth without compromising the absorption. In Fig. 4(a) it can be observed that there is a partial absorptivity drop throughout the desired bandwidth of the absorber until the optimum spacing $S = 6.8$ mm. If

(a)

(b)

(c)
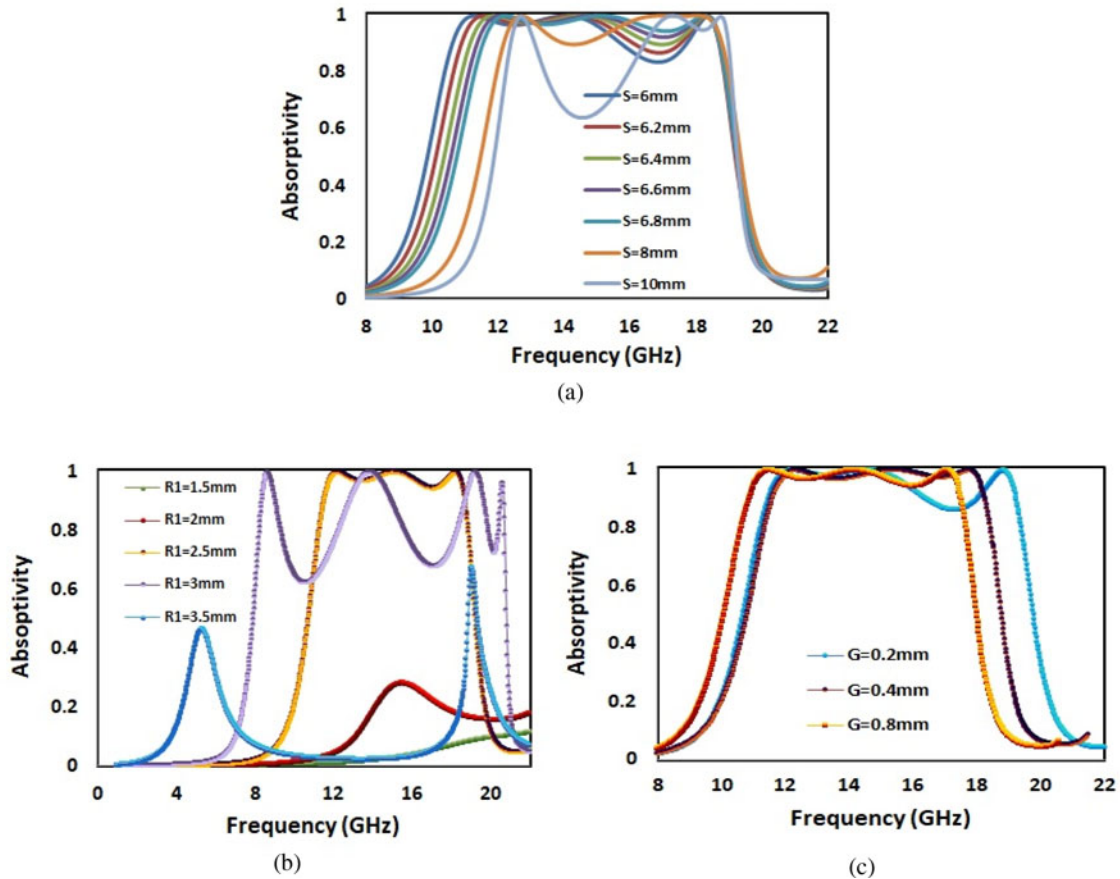
Fig. 4. Parametric analysis of proposed absorber (a) absorptivity response in variance with unit cell spacing "*S*" (b) absorptivity response in variance with outer ring radius "*R1*" (c) absorptivity variation due to split-gap in the outer ring "*G*" at normal incident.


(a)

(b)
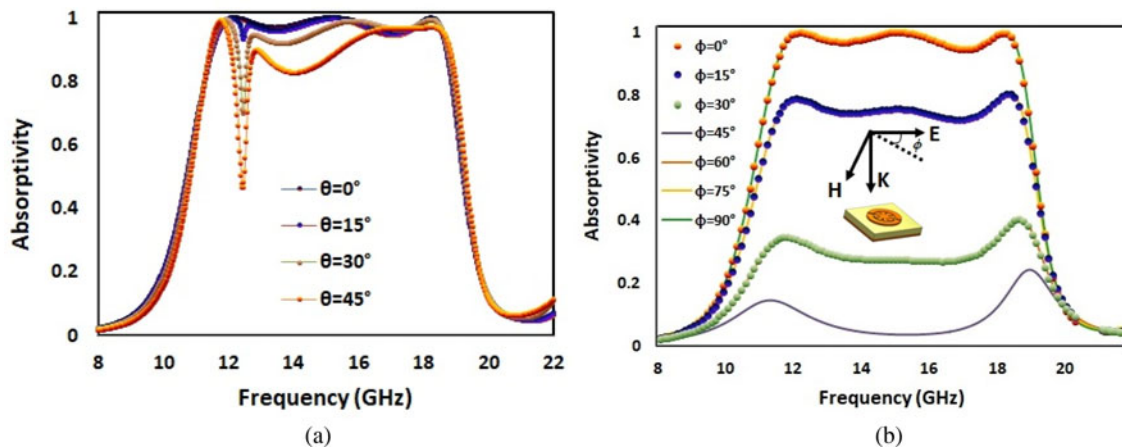
Fig. 5. Absorber Performance (a) shows the variation in the incident angle "*θ*" with polarization angle ϕ = 0°, (b) shows the variation of polarization angle "ϕ" with normal incidence.

the spacing is increased beyond 6.8 mm the bandwidth of the absorber reduces to a large extent along with the absorption level. Furthermore, the iterations done on the outer ring radius R1 as indicated in Fig. 4(b) indicate that the absorptivity and bandwidth are affected by these variations.

It is also clear that the optimum ring radius for the absorber structure is R1 = 2.5 mm having absorptivity above 90%

throughout the bandwidth. Split gaps are very significant as they contribute to the effective capacitance of the absorber resonance and thus can be used for the tuning of the resonator. Figure 4(c) indicates the iterations of a split gap that is optimized to keep the entire bandwidth above 90% absorptivity. It can be observed that if the gap is reduced the performance of the absorber reduces and if the gap is increased the bandwidth of
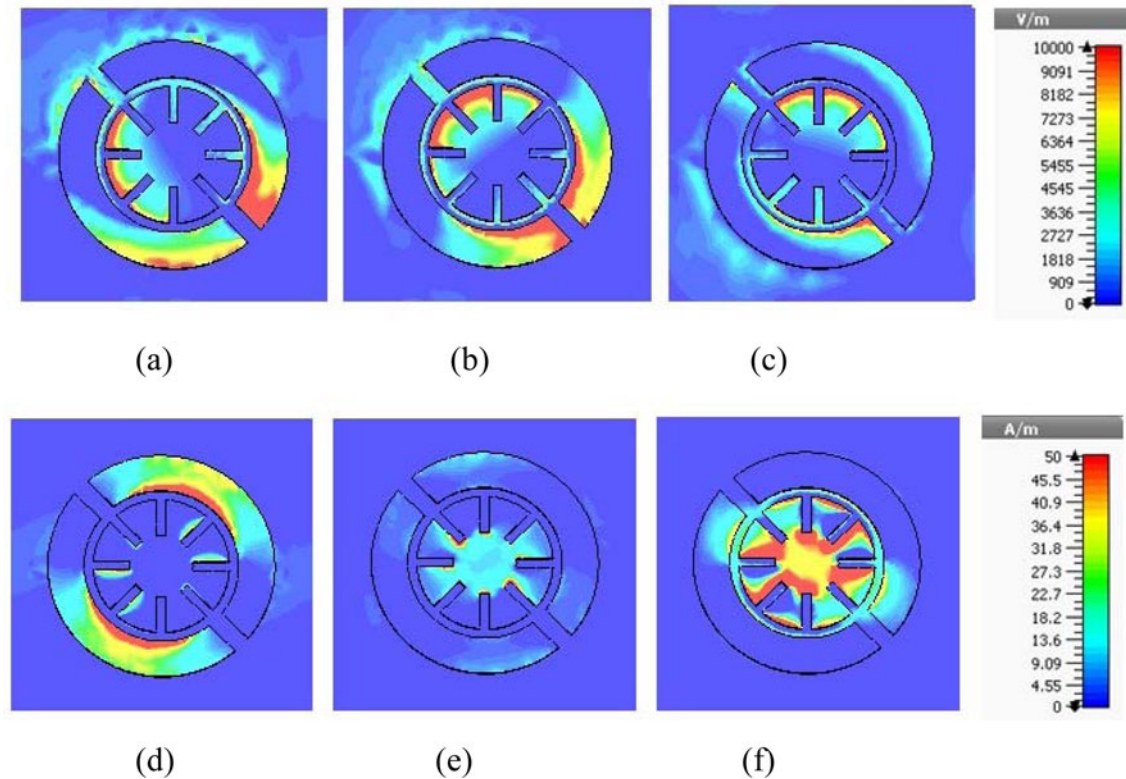
Fig. 6. Electric field distribution at (a) 12.23 GHz, (b) 15.14 GHz & (c) 18.25 GHz. Magnetic field distribution at (d) 12.23 GHz, (e) 15.14 GHz & (f) 18.25 GHz respectively at normal incidence.

the absorber is affected. So, to maintain the performance as well as the bandwidth of the absorber the optimum gap width is $G = 0.4$ mm.

## Absorber performance and structure analysis

After designing the absorber and ensuring the absorptivity, it is very much required to quantify the absorber performance based on the orientation of the absorber as well as the angle at which the absorber receives the electromagnetic waves. The orientation of the absorber termed as the polarization angle is given by ϕ, which agrees that if the absorber orientation changes and there is no variation in absorptivity, the absorber is polarization insensitive. Furthermore, the direction from which the electromagnetic waves are incident is denoted with angle θ, such that $\theta = 0°$, when a wave is an incident normal to the absorber plane. In this section, polarization angle and incident angle are demonstrated with the Floquet ports considered for both TE and TM waves. Figure 5 shows the variation of absorption bandwidth and performance due to the variation in polarization angle (ϕ) and incident angle (θ). It is clear from Fig. 5(a) that the structure holds good reliability when electromagnetic waves are incident at different angles. Incident angle θ is varied from 0 to 45°. It has been observed from the results that more than 80% of the absorptivity is maintained throughout a bandwidth of 12.6–18.7 GHz for an incident angle of 45°. This indicates at the incident angle of 45°, 77% of total bandwidth is maintained for the proposed absorber. Therefore, the absorber is insensitive to the angle of incidence of the approaching electromagnetic wave. Figure 5(b) shows the variation of the polarization angle. The structure is studied for different polarization angles in a range of 0–90° with a step size of 15°, at the

normal incidence in order to inspect its polarization sensitivity. Figure 5(b) shows that absorption decreases gradually with an increase in the polarization angle due to the non-symmetrical geometry of the proposed structure. It is also observed that the absorptivity gradually decreases with an increase in the polarization angles and the minimum value is at 45°. It again increases gradually and reached maximum absorption at 90° polarization angle, showing that the proposed structure is two-fold symmetric. Therefore, the absorptivity is the same at polarization angles $\phi = 0$ and 90°. It can be stated from the results that the proposed absorber is insensitive to incident angle variations and sensitive to polarization angle variations.

The structure of the absorber design comprises a split-ring and is floret-shaped. Figure 6 shows the structure behavior with the approaching electromagnetic wave indicating the electric and magnetic fields. The fields are analyzed using the field monitors in the CST-microwave studio. Figures 6(a) and 6(b) show that at a lower frequency of the entire spectrum i.e. 12.23 GHz, the electric and magnetic fields are majorly contributed by the ring structure. Further moving to the higher frequencies i.e. 15.4 and 18.25 GHz it is observed that the inner floret structure has a significant contribution.

Measurements and results

To validate the designed absorber, the setup has been prepared by placing the horn antenna in front of the fabricated prototype absorber at a distance of 1 m. The fabricated prototype and a large view of the unit cell structure of the designed absorber are shown in Fig. 7(a). The prototype is prepared using a photolithography process with copper-clad laminate. The absorber has been
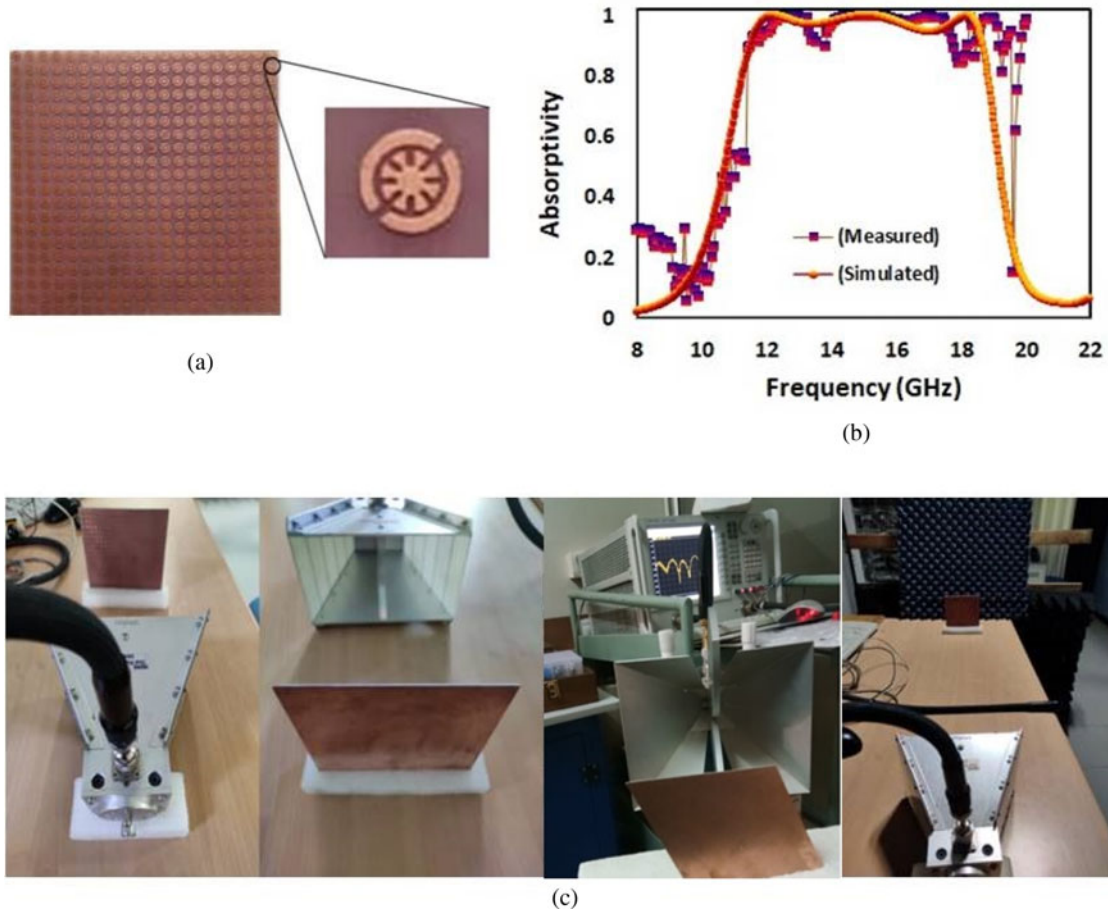
Fig. 7. Measurements: (a) fabricated metasurface absorber sheet and unit cell structure of the prototype absorber (b) Simulated and measured results of metasurface at normal incidence (c) Measurement setup.

Table 2. Comparison with wideband single layer ultrathin metamaterial absorbers

Center frequency (GHz)	Unit cell size (mm)	Unit cell size (operating λ[a])	Thickness (mm)	Substrate layers	Bandwidth (GHz) at 90% absorptivity	Fractional bandwidth
10.05	7.1	$0.238\lambda_0$	2.0	Single	4.4	43%[4]
13.33	26	$0.92\lambda_0$	4.0	Multiple	10.97	107%[11]
13.6	10	$0.31\lambda_0$	7.35	Single	11.5	117%[12]
12.5	7	$0.30\lambda_0$	1.6	Single	5.0	40%[15]
11.2	40.0	$1.5\lambda_0$	0.8	Single	2.85	24.9%[16]
9.97	7.2	$0.24\lambda_0$	1.0	Single	1.15	20%[17]
3.9	10	$0.1\lambda_0$	10	Single	4.12	105%[18]
8.93	9	$0.18\lambda_0$	3.2	Single	5.98	66.9%[19]
14.97	8.4	$0.24\lambda_0$	5	Multiple	21.0[b]	139.6%[20]
15	6.8	$0.37\lambda_0$	1.6	Single	7.4	50% (proposed)

[a]Operating λ and λ_0 is corresponding to center frequency.
[b]At 80% absorptivity.

backed by a wedge-shaped conventional absorber to mitigate undesirable reflections as already shown in Fig. 7(b).

The prototype of the absorber consisting of an array of 20×20 unit cells fabricated on a 1.6 mm thick FR-4 substrate using a photolithography technique and the measurement setup in the laboratory is shown in Fig. 7(c).

Measurement of the reflection coefficient is taken by connecting the setup shown with the vector network analyzer-VNA (Agilent Technologies-N5222A) having a frequency range of 10 MHz to 50 GHz. Figure 7(b) shows the simulated and measured results are in good agreement. Minor deviations are due to fabrication errors or manual errors during measurements [21–23].

Conclusions

A wideband ultra-thin metasurface absorber on a single-layer dielectric has been designed using a split-ring resonator loaded with a floret-shaped patch. A 90% absorptivity is maintained throughout the frequency bandwidth (7.4 GHz). The designed absorber is insensitive to the variation of the incident angle (θ) of the approaching electromagnetic wave. The results have been compared with the existing absorbers in Table 2 which show the superiority of the proposed design and found that the proposed absorber will be a good alternative in Ku-band applications as it is lightweight, inexpensive, and easy to fabricate.

References

1. **Li W, Lin L, Li C, Wang Y and Zhang J** (2019) Radar absorbing combinatorial metamaterial based on silicon carbide/carbon foam material embedded with split square ring metal. *Results in Physics* **12**, 278–286.
2. **Beeharry T, Yahiaoui R, Selemani K and Ouslimani HH** (2018) A dual-layer broadband radar absorber to minimize electromagnetic interference in radomes. *Scientific Reports* **8**, 1–9.
3. **Iwaszczuk K, Strikwerda AC, Fan K, Zhang X, Averitt RD and Jepsen PU** (2012) Flexible metamaterial absorbers for stealth applications at terahertz frequencies. *Optics Express* **20**, 635.
4. **Ghosh S, Bhattacharyya S, Chaurasiya D and Srivastava KV** (2015) An ultra-wideband ultrathin metamaterial absorber based on circular split rings. *IEEE Antennas and Wireless Propagation Letters* **14**, 1172–1175.
5. **Xu B, Gu C, Li Z, Liu L and Niu Z** (2014) A novel absorber with tunable bandwidth based on graphene. *IEEE Antennas and Wireless Propagation Letters* **13**, 822–825.
6. **Sharma A, Panwar R and Khanna R** (2019) Experimental validation of a frequency-selective surface-loaded hybrid metamaterial absorber with wide bandwidth. *IEEE Magnetics Letters* **10**, 1–5.
7. **Fan S and Song Y** (2018) Bandwidth-enhanced polarization-insensitive metamaterial absorber based on fractal structures. *Journal of Applied Physics* **123**, 2018.
8. **Xiong H, Hong JS, Luo CM and Zhong LL** (2013) An ultrathin and broadband metamaterial absorber using multi-layer structures. *Journal of Applied Physics* **114**, 2013.
9. **Costa F, Monorchio A and Manara G** (2016) Theory, design, and perspectives of electromagnetic wave absorbers. *IEEE Electromagnetic Compatibility Magazine* **5**, 67–74.
10. **Yoo M and Lim S** (2014) Polarization-independent and ultra-wideband metamaterial absorber using a hexagonal artificial impedance surface and a resistor-capacitor layer. *IEEE Transactions on Antennas and Propagation* **62**, 2652–2658.
11. **Lim D and Lim S** (2019) Ultra-wideband electromagnetic absorber using sandwiched broadband metasurfaces. *IEEE Antennas and Wireless Propagation Letters* **18**, 1887–1891.
12. **Liu T and Kim SS** (2016) Design of wide-bandwidth electromagnetic wave absorbers using the inductance and capacitance of a square loop-frequency selective surface calculated from an equivalent circuit model. *Optics Communications* **359**, 372–377.
13. **Mishra R, Panwar R and Singh D** (2018) Equivalent circuit model for the design of frequency-selective, terahertz-band, graphene-based metamaterial absorbers. *IEEE Magnetics Letters* **9**, 1.
14. **Agarwal M and Meshram MK** (2018) Metamaterial-based dual-band microwave absorber with polarization-insensitive and wide-angle performance. *AIP Advances* **8**, 1–8.
15. **Khanna Y and Awasthi YK** (2020) Ultra-thin wideband polarization insensitive metasurface absorber for aviation. *Journal of Electronic Materials* **49**, 6410–6416.
16. **Liu Y, Gu S, Luo C and Zhao X** (2012) Ultra-thin broadband metamaterial absorber. *Applied Physics A: Materials Science & Processing* **108**, 19–24.
17. **Ghosh S, Bhattacharyya S, Kaiprath Y and Vaibhav Srivastava K** (2014) Bandwidth-enhanced polarization-insensitive microwave metamaterial absorber and its equivalent circuit model. *Journal of Applied Physics* **115**, 104503-1–104503-5.
18. **Wang Q and Cheng Y** (2020) Compact and low-frequency broadband microwave metamaterial absorber based on meander wire structure loaded resistors. *International Journal of Electronics and Communications (AEÜ)* **120**, 1–8.
19. **Ranjan P, Choubey A, Mahto SK, Sinha R and Barde C** (2019) A novel ultrathin wideband metamaterial absorber for X-band applications. *Journal of Electromagnetic Waves and Applications* **33**, 2341–2353.
20. **Li S-J, Wu P-X, Xu H-X, Zhou Y-L, Cao X-Y, Han J-F, Zhang C, Yang H-H and Zhang Z** (2018) Ultra-wideband and polarization-insensitive perfect absorber using multilayer metamaterials, lumped resistors, and strong coupling effects. *Nanoscale Research Letters* **13**, 386.
21. **Saxena G, Awasthi YK and Jain P** (2021) Design of metasurface absorber for low RCS and high isolation MIMO antenna for radio location & navigation. *International Journal of Electronics and Communications (AEÜ)* **133**, 153680.
22. **Khanna Y and Awasthi YK** (2020) Wideband Ultra-thin Metamaterial Absorber for Ku & K-Band Applications. *IEEE, 7th International Conference on Signal Processing and Integrated Networks (SPIN)*. pp. 367–371.
23. **Saxena G, Yadava RL, Jain P and Awasthi YK** (2020) Tripple Band Polarization Insensitive Ultra Thin Metamaterial Absorber for EMC and RCS Reduction in X-Band Applications. *IEEE, 7th International Conference on Signal Processing and Integrated Networks (SPIN)*. pp. 772–775.

Yogita Khanna received her B.Tech. degree in electronics and communication engineering, from Punjab Technical University, Punjab, India, in 2005, her M.Tech. degree in electronics and communication, from the Thapar Institute of Engineering and Technology, India, in 2008, and completed her Ph.D. from Manav Rachna University, Faridabad, India in 2020. She worked as senior engineer in LG Electronics Pvt. Ltd., Greater Noida, India from 2008 to 2010. She also worked as lecturer at the Thapar Institute of Engineering and Technology, Patiala. Currently, she is working as an Assistant Professor at Manav Rachna University, Faridabad, Haryana. Her main research interests are the design and optimization of metamaterial-based microwave components. Currently, she is working on metamaterial-based absorbers and sensors.

Y. K. Awasthi received his B.Sc. (Electronics) degree from Dr. BRA University, Agra, India in 1999, his M.Sc. (Electronics & Computational Physics) degree from the Institute of Basic Science, Dr. BRA University, Agra, India in 2001, and Ph.D. (RF & Microwave Electronics) from Delhi University, Delhi, in 2012. He was co-operative faculty at the University of Delhi, New Delhi and he was also guest faculty at Central Electronics Engineering Research Institute, Pilani, Rajasthan, India in 2006–2012. He is currently working as a Professor with the Department of Electronics and Communication Engineering, Manav Rachna International Institute of Research and Studies University, Faridabad, India. He has published more than 80 articles in peer-reviewed journals and conferences and he has also filed/published seven patents and published one book chapter. His recent research interest includes modeling of high-frequency passive microwave components, microwave antennas for LTE and 5G applications, meta-material absorbers, sensors & cloaking, study of transient, RF power transfer & energy harvesting, MIMO receiver systems, electrical power systems, etc. He is an Editor-in-Chief in the renowned "*Journal of Sciences and Technology*" and working as a reviewer for several refereed journals such as *IEEE Antennas and Propagation Magazine, IET Microwaves, Antennas, Propagation, IET Electronic Letter, IEEE Access, IEEE Transactions on Antennas & Propagation, AEUE International Journal of Electronics and Communication, Elsevier, Journal of Electromagnetic Waves and Applications (JEMWA), Taylor & Francis, International Journal of Electronics, Taylor & Francis and Applied Computational Electromagnetic Society, ACES*.